The impacts from Sr4La(PO4)3O: Ce3+, Tb3+, Mn2+ phosphor resulting in luminous flux of WLED devices

Huu Phuc Dang[1], Bui Van Hien[2], Nguyen Le Thai[3]
[1]Faculty of Fundamental Science, Industrial University of Ho Chi Minh City, Ho Chi Minh City, Vietnam
[2]Faculty of Mechanical-Electrical and Computer Engineering, School of Engineering and Technology, Van Lang University,
Ho Chi Minh City, Vietnam
[3]Faculty of Engineering and Technology, Nguyen Tat Thanh University, Ho Chi Minh City, Vietnam

Article Info

ABSTRACT

Using the solid-state technique that involves great temperature, we created multiple phosphors $Sr_4La(PO_4)_3O:Ce^{3+}$, Tb^{3+}, Mn^{2+} (abbreviated as SLPO:Ce, Tb, Mn). We then examined their heat consistency, luminescence, as well as energy shift from Ce^{3+} to Tb^{3+} and Mn^{2+}. We can acquire a considerable boost for the faint emission in green generated by Tb^{3+} as well as the emission in red generated by Mn^{2+} via adding the sensitizer Ce^{3+} ions. Through modifying the proportion between Ce^{3+} and Tb^{3+} along with the proportion between Ce^{3+} and Mn^{2+}, it is possible to adjust the chroma of emission. We acquired white illumination which had color coordinates determined as (0.3326, 0.3298) for the testing phosphor $Sr_4La(PO_4)_3O$: $0.12Ce^{3+}$, $0.3Mn^{2+}$. Such result displays the promising efficiency of phosphors SLPO:Ce, Tb, Mn within the white light-emitting diode (WLED) devices.

Corresponding Author:

Bui Van Hien
Faculty of Mechanical-Electrical and Computer Engineering, School of Engineering and Technology
Van Lang University
Ho Chi Minh City, Vietnam
Email: hien.bv@vlu.edu.vn

1. INTRODUCTION

The white light-emitting diode (WLED) devices (short for diodes that generate white illumination) possess many valuable features such as significant time of use, power-economical nature, compactness as well as limited effect on environment, which have made them fairly popular as solid-state illumination generators [1], [2]. Nowadays, for the task of generating white illumination, we would usually integrate one blue InGaN chip with the yellow phosphor YAG:Ce (also known as $Y_3Al_5O_{12}:Ce^{3+}$) [3]. On the other hand, such method has insufficient red-illumination element and thus would yield white illumination with inferior color rendering index (CRI) measured at approximately 70 to 80 and significant correlated color temperature (CCT) measured at approximately 7500 K [4]-[6]. Various new studies focused on examining the red phosphors that are receptive to blue-illumination excitation. The said phosphors include $Na_5Ln(MoO_4)_4$: Eu^{3+} (with Ln being equivalent to La, Gd and Y), CaS: Eu^{2+} [7], $CaAlSiN_3$: Eu^{2+} [8], $K_2SiF_6:Mn^{4+}$ and many others [9], [10]. The WLED devices, based on the said phosphor for conversion, would be able to yield small CCTs as well as great CRIs. On the other hand, we still have to tackle more issues such as considerable production price and low performance for the blue emission caused by potent reabsorption between the phosphors in red and green. As such, there have been a great number of researches that aim at creating one-phase white-illumination phosphor that have desirable performance, longevity and possess the elements of red, green, blue (RGB) on the basis of energy shift (ET) between sensitizers and activator [11], [12]. There is

a great deal of available phosphors to be used in WLED, but treating with Ce^{3+}, Tb^{3+}, or Mn^{2+} ions appear to be usually utilized to generate white illumination via ET for the one-phase phosphors [13]. Ce^{3+} possesses $4f^1 5d^0$ ground state and $4f^0 5d^1$ excited state. As a result, it displays standard balance allowed 5d-4f electronic shifts. The Ce^{3+} energy allocation has a strong connection to the host lattice, and as such it is possible for the the emission from the shift from 5d to 4f to occur when there is a limit consisting of big wavelengths. The Tb^{3+} and Mn^{2+} ions would be usually utilized to add green and red elements. But the ions' excitation bands between ultraviolet (UV) and observable area would be particularly faint, which is the result of the forbidden 4f-4f shift in Tb^{3+} as well as the $^4T_1$-$^6A_1$ shift in Mn^{2+} [14], [15]. If we need to boost the Tb^{3+} and Mn^{2+} absorption within the UV region, there is a common technique we can utilize which involves adding an effective sensitizer like Ce^{3+} and shifting the absorbed excitation energy from 5d state in Ce^{3+} to $^5D_{3,4}$ state in Tb^{3+} or 4G state in Mn^{2+} [16], [17]. After that, it is possible to acquire one-phase phosphors with adjustable chromas, small production price, desirable chroma generation as well as great luminescence performance [18], [19]. Some have claimed that apatites could become remarkable host substances in phosphors as they offer decent consistency, both physically and chemically [20]. $Sr_4La(PO_4)_3O$ (SLPO) is isomorphic to apatite. It also has two cation places: a nine-fold coordination 4f location accompanied by C3 spot symmetry as well as a seven-fold coordination 6h location accompanied by C5 spot symmetry [21]. An earlier studied performed by us examined the phosphors SLPO: Eu^{3+}/Tb^{3+}/Ce^{3+} [22]. For our research, SLPO: Ce^{3+} would be integrated with Mn^{2+} or Tb^{3+}. It is possible to acquire a green emission peak from Tb^{3+} under the wavelength of 539 nm as well as a red emission band from Mn^{2+} under a top wavelength of 605 nm via energy shift. We examined the features of photoluminescence along with energy shift between Ce^{3+} and Tb^{3+} as well as Ce^{3+} and Mn^{2+}. For the purpose of generating adjustable chromas going from blue to green then white, we can modify the doping concentration for Tb^{3+} and Mn^{2+}. This means that it would be potentially useful for UV-WLED devices.

2. COMPUTATIONAL SIMULATION

2.1. Experimental

We created various compounds of the phosphors $Sr_4La_{1-x-y}(PO_4)_3O$: xCe^{3+}, yTb^{3+} and $Sr_{4-z}La_{1-x}(PO_4)_3O$: xCe^{3+}, zMn^{2+} using the standard solid-state technique. The substances used for the preparation are $SrCO_3$ (99%), $(NH_4)_2HPO_4$ (99%), La_2O_3 (99.99%), Tb_4O_7 (99.99%), $MnCO_3$ (99%), CeO_2 (99.99%). We added 2 wt% Li_2CO_3 (99%), which acted like flux. We mixed the determined amounts of the said substances and grinded the blend using agate mortar. We heated the blend in the air under the temperature of 600°C for three hours. Next, we grinded then calcinated the blend under the temperature of 1200°C for five hours under a declining atmosphere (N_2: H_2=95:5).

We assessed the clarity of the phase via the ARL X'TRA powder X-ray diffractometer (abbreviated as XRD) accompanied by Cu Kα emission, with λ equal to 1.5406 Å which worked under an amperage of 35 miliampe and a voltage of 40 kilovolt. We acquired the DRS (short for diffuse reflection spectrum) using the UV/visible spectrometer (UV-3600, SHIMADZU) that utilizes $BaSO_4$ under the wavelength limit of 200 nm to 700 nm. We assessed the forms of the created substances using an area emission scanning electronmicroscope. We detected the photoluminescence excitation spectroscopy (PLE) spectrum (known as radiancy excitation) and photoluminescence spectroscopy (PL) spectrum (known as radiancy) using the Edinburgh FS5 fluorescence spectrophotometer possessing an optical source which is xenon lamp working under a wattage of 150 W. We determined the dependence of temperature using the FS5 spectrofluorometer structure, then placed the substances over a heating apparatus with the heating range of 20°C–200°C. We acquired the photoluminescence outer quantum using a sphere of the FS5 spectrophotometer. We assessed the duration of fluorescence using the Edinburgh FLS 920 Fluorescence Spectrophotometer.

2.2. Luminescence features and energy shift of the phosphor SLPO:Ce^{3+},Tb^{3+}

We assessed the SLPO's light bandgap by acquiring its absorption spectra from reflection spectra using the Kubelka-Munk as shown in (1) [23].

$$F(R) = \frac{(1-R)^2}{2R} = K/S \tag{1}$$

As shown in (1), *R, K, S* indicate the reflection, absorption, diffusing factor. According to the Tauc expression demonstrates the relationship between the bandgap E_g and a substance's linear coefficient α [24].

$$\alpha hv \propto (hv - E_g)^{n/2} \tag{2}$$

As shown in (3), v represents the energy of photon, n is equal to the values 1, 2, 3, 4, 6, which represents the direct allowed shifts, the substances that are not metals, the direct forbidden shifts, the non-direct allowed shifts and the non-direct forbidden shifts [25]. K, which represents the absorption coefficient, is equivalent to 2α if the substance disperses randomly. With the scattering coefficient S being a constant corresponding to a wavelength, we can utilize (3), based on (1) and (2).

$$[F(R)hv]^2 \propto (hv - E_g)^n \tag{3}$$

Between $[F(R)hv]^2$, $[F(R)hv]$, $[F(R)hv]^{2/3}$, $[F(R)hv]^{1/2}$, $[F(R)hv]^{1/3}$ through hv, we can acquire the most desirable linear fitting around the absorption rim when n is equal to 2. Figure 1 displays $[F(R)hv]$ and hv. When we extrapolate the linear fir to $[F(R)hv]$ being equal to zero, we can acquire the light bandgap of SLPO as 3.85 eV.

We can determine the efficacy of ET (also known as η_{ET}) between a sensitizer and activator using:

$$\eta_{ET} = 1 - \frac{I_s}{I_{s0}} \tag{4}$$

As shown in (4), I_s and I_{s0} represents the sensitizer's (Ce^{3+}) intensities under the appearance and the lack of activator, which is either Tb^{3+} or Mn^{2+}. When the concentration of the activator goes up, the range separating the sensitizer and the activator goes down, which boosts the ET efficacy. When y at 0.01 value reaches 0.15 for SLPO: $0.12Ce^{3+}$, yTb^{3+}, η_{ET} at 11.28% receives a steady boost, reaching 34.66%.

We determined and examined the Ce^{3+} fluorescence decay curves observed under the wavelength of 469 nm for SLPO: $0.12Ce^{3+}$, yTb^{3+} affected by a 310-nm excitation, so that we could verify the ET activities between the Ce^{3+} and Tb^{3+} ions of the SLPO host. The Ce^{3+} decay curves drift from the sole exponential one. This activity is encouraged when the concentration of Tb^{3+} goes up. As the decay curves do not appear to be exponential, we can identify the decay activity in the substances using the fluorescence duration, which is determined by (5).

$$\tau = \frac{\int_0^\infty I(t)t\,dt}{I(t)dt} \tag{5}$$

As shown in (5), $I(t)$ indicates the intensity of fluorescence for t, which represents time. Using the formula, the values of standard Ce^{3+} duration of SLPO: $0.12Ce^{3+}$, yTb^{3+} would be determined as: 50.3, 48.7, 45.9, 43.4, 40.0, 35.9 ns. These values correspond to the y values: 0, 0.01, 0.03, 0.07, 0.1, 0.15. When the concentration of Tb^{3+} goes up, the decay duration of Ce^{3+} goes down, which suggests that the energy shift exists among ions of Ce^{3+} as well as Tb^{3+}. In addition, we can determine the efficacy of ET, represented by η_{ET}, between Ce^{3+} and Tb^{3+} using (6).

$$\eta_{ET} = 1 - \frac{\tau_s}{\tau_{s0}} \tag{6}$$

We utilize the expression in (7), on the basis of ET expression by Dexter and expression of Reisfeld, to examine how the ET works between Ce^{3+} and Tb^{3+} for SLPO.

$$\frac{\eta_0}{\eta} \propto C^{n/3} \tag{7}$$

Based on ET hypothesis of Dexter, we can determine the critical range (R_c) separating the sensitizer and the receiver for the ET process using the overlay of spectrum technique. When it comes to the dipole-to-dipole interaction, we can determine R_c using (8).

$$R_C^6 = 0.63 X 10^{28} Q_A \int \frac{f_S(E)F_A(E)}{E^4} dE \tag{8}$$

As shown in (8), Q_A is equal to 4.8 x $10^{-16}f_d$, which represents the absorption factor in Tb^{3+}. f_d indicates the oscillate power for the light absorption shift over the ion that receives energy (equal to 0.3 x 10^{-6} in the case of Tb^{3+}). E, measured in eV, represents the energy that participates in the shift. $\int \frac{f_S(E)F_A(E)}{E^4} dE$ indicates intersection of spectrum among the standard shape functions for the emission band of the sensitizer, represented by $f_s(E)$, and the excitation band of the acceptor, represented by $F_A(E)$. It is possible to acquire E using the formula $\int f_s(E)dE = \int F_A(E)dE = 1$. We found out that E is approximately 0.0188 eV^{-4}. R_c would be roughly 5.08 Å, similar to the values that were examined earlier. For example, 5.8 Å for $Ca_8MgLu(PO_4)_7$: Ce^{3+}, Tb^{3+} or 7.1 Å for $Ca_3La_6(SiO_4)_6$: Ce^{3+}, Tb^{3+}. Such outcome would match the earlier

researches as well. According the said researches, R_c would be limited around 5 Å to 8 Å. This is because the ET would only occur in the closest surroundings within the crystal lattice when the shift occurs between a wide-band emitter and a thin line absorber.

An multiple chips (multi- chip white LEDs (MCW-LEDs)) device was made in the LightTools 9.0 software via Monte Carlo method and contains phosphor sheet as well as level silicone sheets. The making process includes certain main steps. Initially, we have to identify as well as construct the design as well as illumination qualities for the device. Afterwards, the task is to adjust the phosphor compound's illumination effects by varying the concentrations of SLPO:Ce, Tb, Mn. For the task of examining the way YAG:Ce^{3+} and SLPO:Ce, Tb, Mn phosphor mixing might influence the performance of MCW-LED lights, we must generate specific contrasts. It is needed to examine two kinds of substances at mean CCT levels reaching 3,000 K, 4,000 K, as well as 5,000 K, two-film distant phosphor. In Figure 1, we can see a depiction of MCW-LED device having daubed with phosphor composition at an elevated CCT (8,500 K). It is also indicated that the making of the device may ignore SLPO:Ce, Tb, Mn. The parameters for the reflector are 8 mm, 2.07 mm, and 9.85 mm for length of base, height and length of highest exterior, respectively. The protective-coating phosphor composition would be covered above nine chips, with all of them having a breadth reaching 0.08 nm. All chips have a square shape, a length of 1.14 mm along with a height of 0.15 mm. The chips would be connected to cavity of the reflector. The radiative light from each chip is measured at 1.16 W, under an apex wavelength reaching 453 nm.

Figure 1. Photograph of WLEDs

3. RESULTS AND DISCUSSION

The SLPO: Ce, Tb, Mn green phosphorus concentration content appears to be inverse to the concentration of yellow phosphorus YAG:Ce^{3+} in Figure 2, indicating two meanings: initially, sustaining median CCT values; secondly, the absorption as well as dispersion for the phosphor sheets within the WLED device. As a consequence, the hue performance, along with lumen generation, becomes impacted. So, the SLPO:Ce, Tb, Mn content controls the chromatic performance of WLEDs. As the concentration of YAG:Ce^{3+} rises (2%-20% Wt.), the YAG:Ce^{3+} content fell to retain the mean CCT values. This phenomenon also happens to WLED devices with CCT limit of 5600 K - 8500 K.

Figure 3 illustrates the way the concentration for SLPO:Ce, Tb, Mn may affect the WLED device's light. Choosing a correct content of SLPO:Ce, Tb, Mn is crucial and will be decided by the aims of producers. Having desirable color output, WLED devices will suffer from an insignificant penalty for illumination. The mixture of spectrum zones results in white illumination, demonstrated in Figure 3. The pictures depict the light under CCT values measured at 5600 K, 6600 K, 7000 K, along with 8500 K. The two regions of the optic spectra with wavelength ranges (420-480 nm along with 500-640 nm) reveal that the illumination degree surges along with SLPO:Ce, Tb, Mn content. A growth of the the dual-line emission spectrum displays an increment for light performance. On the other hand, the dispersion for blue illumination from the WLED device exhibits greater activity, showing greater dispersion for the phosphor film as well as the device, improving hue uniformity. Having that outcome might be critical for the application of SLPO:Ce, Tb, Mn. Controlling hue consistency for one distant phosphor setting under great temperatures, in particular, may require a lot of efforts. The team's investigation determined the capacity of SLPO:Ce, Tb, Mn at 5600 K as well as 8500 K, to augment the hue efficiency within WLED apparatuses.

Our research has managed to verify the lumen output for the mentioned phosphor setting. With the SLPO:Ce, Tb, Mn content rising (2%-20% wt.) in Figure 4, the lumen sees a substantial surge. The chroma aberration saw a substantial decline as the SLPO:Ce, Tb, Mn content surges under three median CCT values in Figure 5. The absorption from the red phosphor sheet clarifies one such occurrence. When the blue illumination emitted via the chip in LED gets assimilated via the grains of blue phosphor, it will be

transmuted, becoming green illumination. On the other hand, the SLPO:Ce, Tb, Mn grains will also assimilate yellow illumination as well. With the material's assimilation features, the absorptivity from the blue ray made via said chip would offer greater performance, surpassing mentioned absorptivities. With the presence of SLPO:Ce, Tb, Mn, the green component in the WLED apparatus would be enhanced and would improve color consistency. Color homogeneity is regarded as a critical characteristic in todays modern WLED lamps. Achiving greater color consistency will surge WLED's value. Regardless, SLPO:Ce, Tb, Mn may help cut down costs, potentially leading to wide use.
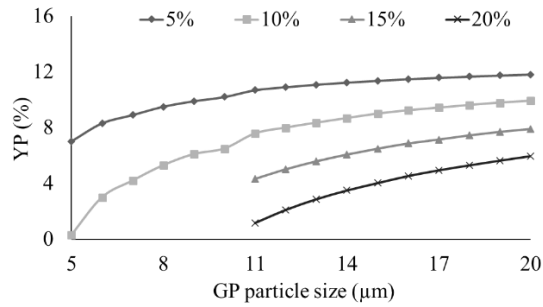
Figure 2. Sustaining standard CCT level through modifying the concentration of phosphor
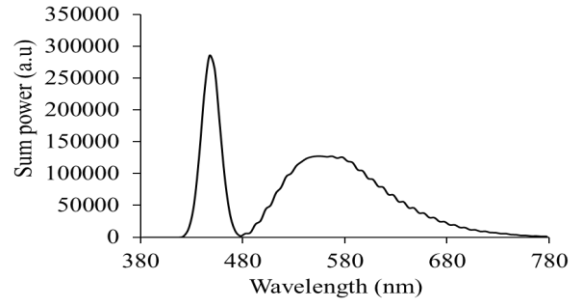
Figure 3. The emission spectrum in WLED device under 5000K with respective concentrations of SLPO:Ce, Tb, Mn
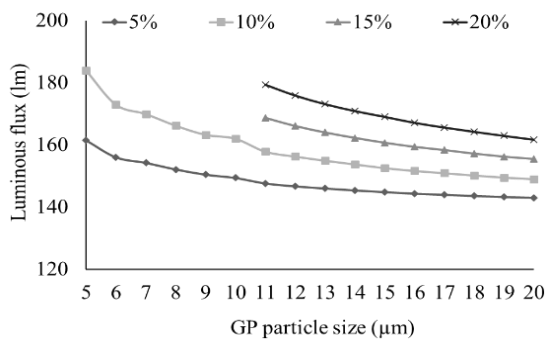
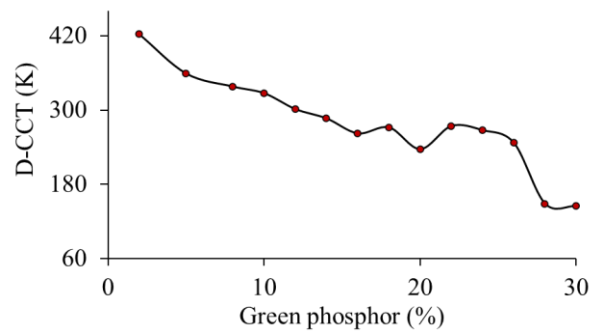Figure 4. The lumen from the WLED device correlating with respective contents of SLPO:Ce, Tb, Mn

Figure 5. The hue divergence within the WLED device with respective concentrations of SLPO:Ce, Tb, Mn

Hue consistency would be among certain factors that influence color output in WLED apparatuses. Desirable color consistency is merely a requirement for color output. Earlier investigations suggested one element for the purpose of gauging chromatic rendition as well as hue output. When CRI assesses illumination striking an item, its genuine chroma can be seen. Lacking color uniformity results from the dominating green illumination between the primary hues (blue, yellow, as well as green). This will alter the WLED device's color efficiency and reduce color consistency. Judging Figure 6, using one SLPO:Ce, Tb, Mn sheet, CRI goes down slightly, which is a mere small drawback. Unlike CRI, CQS would be harder to get and is favored. CQS considers certain factors: CRI, watcher preference, along with hue coordination and seems to be an effective as well as universal factor influencing color efficiency. The rise in CQS accompanied by the phosphor film SLPO:Ce, Tb, Mn is displayed by Figure 7. Additionally, as SLPO:Ce, Tb, Mn content surges, CQS hardly displays any significant shift if the content becomes below 10% wt. In case of 10% wt. or greater, CRI and CQS face noticeable penalties owing to the considerable chroma waste resulting from excessive green hue. The utilization of SLPO:Ce, Tb, Mn would require appropriately determining its concentration.
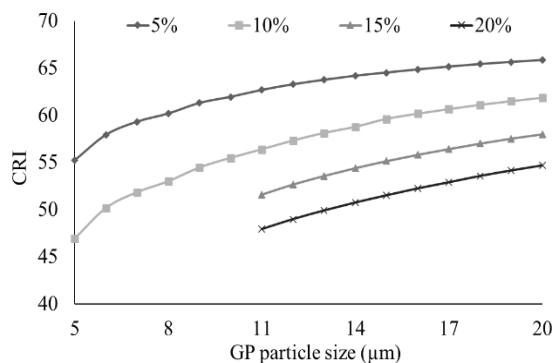
Figure 6. The CRI values (color rendering index) in the WLED device with respective concentrations of SLPO:Ce, Tb, Mn
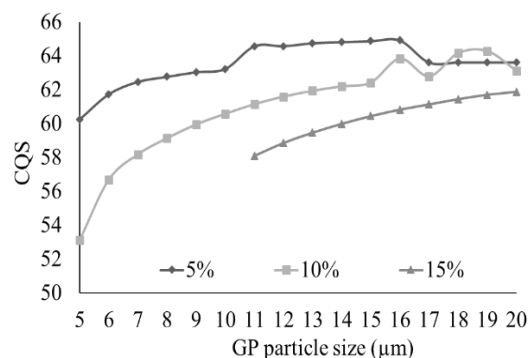

Figure 7. The CQS values (color quality scale) in the WLED device with respective concentrations of SLPO:Ce, Tb, Mn

4. CONCLUSION

$Sr_4La(PO_4)_3O:Ce^{3+}$, Tb^{3+}, Mn^{2+} (SLPO:Ce, Tb, Mn) has the ability to alter illumination features for the double-sheet phosphor layout, as proven herein. By the Monte Carlo method, it is demonstrated that SLPO:Ce, Tb, Mn will raise hue consistency for WLED devices under 5,000 K along with 8,500 K. Our investigation achieved our aim by augmenting hue output along with lumen. On the other hand, CRI as well as CQS drawbacks were not avoided. If the SLPO:Ce, Tb, Mn content is excessive, these factors suffer from a huge penalty. Consequently, based on the manufacturer's objectives, it would be necessary to pick a correct content degree of phosphor. The findings from our study may provide better insight into acquiring greater hue consistency along with lumen for WLED devices.

ACKNOWLEDGEMENTS

REFERENCES
[1]   W. J. Kim *et al.*, "Improved angular color uniformity and hydrothermal reliability of phosphor-converted white light-emitting diodes by using phosphor sedimentation," *Optics Express*, vol. 26, no. 22, p. 28634, Oct. 2018, doi: 10.1364/oe.26.028634.
[2]   H. Yang *et al.*, "'Giant' quantum dots encapsulated inside a freeform lens," *Applied Optics*, vol. 57, no. 35, p. 10317, Dec. 2018, doi: 10.1364/AO.57.010317.
[3]   X. Li, B. Hussain, L. Wang, J. Jiang, and C. P. Yue, "Design of a 2.2-mW 24-Mb/s CMOS VLC Receiver SoC With Ambient Light Rejection and Post-Equalization for Li-Fi Applications," *Journal of Lightwave Technology*, vol. 36, no. 12, pp. 2366–2375, Jun. 2018, doi: 10.1109/JLT.2018.2813302.
[4]   X. Ding *et al.*, "Improving the optical performance of multi-chip LEDs by using patterned phosphor configurations," *Optics Express*, vol. 26, no. 6, p. A283, Mar. 2018, doi: 10.1364/oe.26.00a283.
[5]   E. Robledo *et al.*, "Coregistered and segmented tissue oxygenation maps onto white light images of diabetic foot ulcers," in *Optics InfoBase Conference Papers*, 2018, vol. Part F91-TRANSLATIONAL 2018, p. JW3A.44, doi: 10.1364/TRANSLATIONAL.2018.JW3A.44.
[6]   A. Keller, P. Bialecki, T. J. Wilhelm, and M. K. Vetter, "Diffuse reflectance spectroscopy of human liver tumor specimens - towards a tissue differentiating optical biopsy needle using light emitting diodes," *Biomedical Optics Express*, vol. 9, no. 3, p. 1069, Mar. 2018, doi: 10.1364/boe.9.001069.
[7]   L. Yang, Q. Zhang, F. Li, A. Xie, L. Mao, and J. Ma, "Thermally stable lead-free phosphor in glass enhancement performance of light emitting diodes application," *Applied Optics*, vol. 58, no. 15, p. 4099, May 2019, doi: 10.1364/ao.58.004099.
[8]   H.-Y. Yu *et al.*, "Solar spectrum matching with white OLED and monochromatic LEDs," *Applied Optics*, vol. 57, no. 10, p. 2659, Apr. 2018, doi: 10.1364/ao.57.002659.
[9]   N. Anous, T. Ramadan, M. Abdallah, K. Qaraqe, and D. Khalil, "Impact of blue filtering on effective modulation bandwidth and wide-angle operation in white LED-based VLC systems," *OSA Continuum*, vol. 1, no. 3, p. 910, Nov. 2018, doi: 10.1364/osac.1.000910.
[10]   P. Zhu, H. Zhu, G. C. Adhikari, and S. Thapa, "Spectral optimization of white light from hybrid metal halide perovskites," *OSA Continuum*, vol. 2, no. 6, p. 1880, Jun. 2019, doi: 10.1364/osac.2.001880.
[11]   H. Yuce, T. Guner, S. Balci, and M. M. Demir, "Phosphor-based white LED by various glassy particles: control over luminous efficiency," *Optics Letters*, vol. 44, no. 3, p. 479, Feb. 2019, doi: 10.1364/ol.44.000479.
[12]   G. Liu, W. Hou, and M. Han, "Unambiguous Peak Recognition for a Silicon Fabry-Pérot Interferometric Temperature Sensor," *Journal of Lightwave Technology*, vol. 36, no. 10, pp. 1970–1978, May 2018, doi: 10.1109/JLT.2018.2797202.
[13]   H.-L. Ke *et al.*, "Lumen degradation analysis of LED lamps based on the subsystem isolation method," *Applied Optics*, vol. 57, no. 4, p. 849, Feb. 2018, doi: 10.1364/ao.57.000849.

[14] L. Xiao, C. Zhang, P. Zhong, and G. He, "Spectral optimization of phosphor-coated white LED for road lighting based on the mesopic limited luminous efficacy and IES color fidelity index," *Applied Optics*, vol. 57, no. 4, p. 931, Feb. 2018, doi: 10.1364/ao.57.000931.

[15] H. Lee, S. Kim, J. Heo, and W. J. Chung, "Phosphor-in-glass with Nd-doped glass for a white LED with a wide color gamut," *Optics Letters*, vol. 43, no. 4, p. 627, Feb. 2018, doi: 10.1364/ol.43.000627.

[16] Q. Xu, L. Meng, and X. Wang, "Nanocrystal-filled polymer for improving angular color uniformity of phosphor-converted white LEDs," *Applied Optics*, vol. 58, no. 27, p. 7649, Sep. 2019, doi: 10.1364/ao.58.007649.

[17] J. Chen, B. Fritz, G. Liang, X. Ding, U. Lemmer, and G. Gomard, "Microlens arrays with adjustable aspect ratio fabricated by electrowetting and their application to correlated color temperature tunable light-emitting diodes," *Optics Express*, vol. 27, no. 4, p. A25, Feb. 2019, doi: 10.1364/oe.27.000a25.

[18] G. Zhang, K. Ding, G. He, and P. Zhong, "Spectral optimization of color temperature tunable white LEDs with red LEDs instead of phosphor for an excellent IES color fidelity index," *OSA Continuum*, vol. 2, no. 4, p. 1056, Apr. 2019, doi: 10.1364/osac.2.001056.

[19] B. Zhao, Q. Xu, and M. R. Luo, "Color difference evaluation for wide-color-gamut displays," *Journal of the Optical Society of America A*, vol. 37, no. 8, p. 1257, Aug. 2020, doi: 10.1364/josaa.394132.

[20] Q. Xu, B. Zhao, G. Cui, and M. R. Luo, "Testing uniform colour spaces using colour differences of a wide colour gamut," *Optics Express*, vol. 29, no. 5, p. 7778, Mar. 2021, doi: 10.1364/oe.413985.

[21] Y. J. Park *et al.*, "Development of high luminous efficacy red-emitting phosphor-in-glass for high-power LED lighting systems using our original low Tg and Ts glass," *Optics Letters*, vol. 44, no. 24, p. 6057, Dec. 2019, doi: 10.1364/ol.44.006057.

[22] M. Royer, "Evaluating tradeoffs between energy efficiency and color rendition," *OSA Continuum*, vol. 2, no. 8, p. 2308, Aug. 2019, doi: 10.1364/osac.2.002308.

[23] H. Jia *et al.*, "High-transmission polarization-dependent active plasmonic color filters," *Applied Optics*, vol. 58, no. 3, p. 704, Jan. 2019, doi: 10.1364/ao.58.000704.

[24] Y. Liang *et al.*, "Phosphor-in-glass (PIG) converter sintered by a fast Joule heating process for high-power laser-driven white lighting," *Optics Express*, vol. 29, no. 10, p. 14218, May 2021, doi: 10.1364/oe.419633.

[25] P. Zhu, H. Zhu, G. C. Adhikari, and S. Thapa, "Design of circadian white light-emitting diodes with tunable color temperature and nearly perfect color rendition," *OSA Continuum*, vol. 2, no. 8, p. 2413, Aug. 2019, doi: 10.1364/osac.2.002413.

BIOGRAPHIES OF AUTHORS

Huu Phuc Dang ⓘ 🅖 SC Ⓟ received a Physics Ph.D degree from the University of Science, Ho Chi Minh City, in 2018. Currently, he is a lecturer at the Faculty of Fundamental Science, Industrial University of Ho Chi Minh City, Ho Chi Minh City, Vietnam. His research interests include simulation LEDs material, renewable energy. He can be contacted at email: danghuuphuc@iuh.edu.vn.

Bui Van Hien ⓘ 🅖 SC Ⓟ is a lecturer at the Faculty of Engineering, Van Lang University, Ho Chi Minh City, Viet Nam. His research interests are Optoelectronics (LED), Power transmission and Automation equipment. He can be contacted at email: hien.bv@vlu.edu.vn.

Nguyen Le Thai ⓘ 🅖 SC Ⓟ received his BS in Electronic engineering from Danang University of Science and Technology, Vietnam, in 2003, MS in Electronic Engineering from Posts and Telecommunications Institute of Technology, Ho Chi Minh, Vietnam, in 2011 and PhD degree of Mechatronics Engineering from Kunming University of Science and Technology, China, in 2016. He is a currently with the Nguyen Tat Thanh University, Ho Chi Minh City, Vietnam. His research interests include the renewable energy, optimisation techniques, robust adaptive control and signal processing. He can be contacted at email: nlthai@nttu.edu.vn.